

Magnetization Studies on Superconducting Vanadium Gallium

D. L. Decker and H. L. Laquer

Citation: *Journal of Applied Physics* **40**, 2817 (1969); doi: 10.1063/1.1658081

View online: <http://dx.doi.org/10.1063/1.1658081>

View Table of Contents: <http://scitation.aip.org/content/aip/journal/jap/40/7?ver=pdfcov>

Published by the [AIP Publishing](#)

Articles you may be interested in

[Electrical resistivity study of La, B doped nanocrystalline superconducting vanadium nitride](#)

J. Appl. Phys. **91**, 6051 (2002); 10.1063/1.1461057

[Nuclear magnetic resonance studies on the surface magnetism of vanadium ultrafine particles \(abstract\)](#)

J. Appl. Phys. **75**, 5903 (1994); 10.1063/1.355556

[Jahn–Teller Distortion: Magnetic Studies of Vanadium Tetrachloride](#)

J. Chem. Phys. **48**, 5544 (1968); 10.1063/1.1668254

[Anomalous Magnetic Behavior of Superconducting Vanadium and Niobium](#)

J. Appl. Phys. **39**, 2159 (1968); 10.1063/1.1656515

[Magnetic Resonance Studies of Lithium Vanadium Bronze](#)

J. Chem. Phys. **37**, 220 (1962); 10.1063/1.1701308

High-Voltage Amplifiers

- Voltage Range from $\pm 50\text{V}$ to $\pm 60\text{kV}$
- Current to 25A

Electrostatic Voltmeters

- Contacting & Non-contacting
- Sensitive to 1mV
- Measure to 20kV



ENABLING RESEARCH AND
INNOVATION IN DIELECTRICS,
ELECTROSTATICS,
MATERIALS, PLASMAS AND PIEZOS



www.trekinc.com

TREK, INC. 190 Walnut Street, Lockport, NY 14094 USA • Toll Free in USA 1-800-FOR-TREK • (t):716-438-7555 • (f):716-201-1804 • sales@trekinc.com

Magnetization Studies on Superconducting Vanadium-Gallium*

D. L. DECKER† AND H. L. LAQUER

Los Alamos Scientific Laboratory, University of California, Los Alamos, New Mexico 87544

(Received 22 November 1968; in final form 20 February 1969)

The temperature dependence of the critical fields of V_3Ga has been measured up to 70 kOe using ac and dc magnetization techniques. For a material with a transition width of 26 mdeg at a transition temperature, T_c , of 14.19°K, one calculates from the slope ($dH_{c2}/dT = -43.2$ kOe/deg) and curvature of the H_{c2} vs T curve, the Ginzburg-Landau parameter, $\kappa = 40 \pm 2$, the Pauli paramagnetism parameter $\alpha = 2.28 \pm 0.04$, and the spin-orbit scattering constant $\lambda_{so} = 0.6 \pm 0.1$. No evidence for H_{c3} was detected and the experimentally difficult upper limit to H_{c1} appears to be about three times as large as calculated from the theories.

I. INTRODUCTION

The intermetallic compound V_3Ga and its superconductivity were discovered by Matthias, Wood, Corenzwit, and Bala.¹ The material is a high-field, type II superconductor with transition temperatures T_c ranging from 14.2° to 16.8°K.²⁻⁴ These variations may be caused by slight differences in composition and in heat treatment during or after formation of the compound. Several properties of superconducting V_3Ga have been measured near T_c ⁵⁻⁷ and observations of the upper critical field over an extended temperature range have also been published.⁸ This work indicates, as also noted by the present authors,⁹ that the experimental upper critical field, H_{c2} , is reduced below the Ginzburg-Landau-Abrikosov-Gorkov (GLAG) upper critical field, H_{c2}^* , by the effect of Pauli spin paramagnetism in the normal state.¹⁰ However, recent experimental¹¹ and theoretical¹² studies suggest that for some high-field superconductors spin-orbit scattering in the superconducting state may partially offset the effect of Pauli spin paramagnetism.

Both dc and high sensitivity ac techniques were used to determine the magnetic properties of hollow cylinders of superconducting V_3Ga in dc magnetic fields up to

70 kOe. The magnetization curves are similar to those of other tubular samples of type II superconductors as measured by Kim, Hempstead, and Strnad¹³ and interpreted by Anderson's¹⁴ flux creep mechanism. Since, according to this model the motion of flux cannot be instantaneous, slight ac frequency effects should be and have been observed. However, the present paper is limited to "steady-state" magnetization curves, critical currents, the various critical fields, and to an analysis of their temperature dependence, leaving frequency effects on flux motion to another article.

II. EXPERIMENTAL

The vanadium-gallium samples studied in this work were obtained as small arc-melted buttons from Professor B. T. Matthias. They were used as received with no further heat treatment, but there were variations in transition temperatures and widths. We selected the sample with the narrowest transition as being indicative of the greatest homogeneity. The sample was fabricated by spark cutting into a hollow cylinder 8.13-mm long, 2.49-mm o.d., and 1.70-mm i.d.

The experiments were performed with the Los Alamos liquid-hydrogen-cooled solenoid¹⁵ capable of producing 80 kOe in a 5-cm-diam low-temperature core. The field calibration was accurate to better than 1%. The magnetic field was controlled by an integrating feedback circuit¹⁶ and could be held constant or swept at any desired rate up to 10 kOe/sec.

Two cryostats were used. The first was a simple liquid-hydrogen bath in which the temperature was taken from the hydrogen vapor pressure, using the equation given by Weber *et al.*¹⁷ based upon the NBS-1955 scale. The second apparatus was a thermally floating helium-cooled copper capsule capable of operating in the temperature range between 2° and 30°K.¹⁸ The temperature of the capsule could be maintained

* Work performed under the auspices of the U.S. Atomic Energy Commission.

† Visiting Staff Member at Los Alamos. Permanent address: Dept. of Physics, Brigham Young University, Provo, Utah.

¹ B. T. Matthias, E. A. Wood, E. Corenzwit, and V. B. Bala, *J. Phys. Chem. Solids* **1**, 188 (1956).

² P. S. Swartz, H. R. Hart, Jr., and R. L. Fleischer, *Appl. Phys. Lett.* **4**, 71 (1964).

³ J. H. Wernick *et al.*, in *High Magnetic Fields*, H. H. Kolm *et al.*, Eds. (John Wiley & Sons, Inc., New York, 1962), p. 609.

⁴ W. E. Blumberg, J. Eisinger, V. Jaccarino, and B. T. Matthias, *Phys. Rev. Lett.* **5**, 149 (1960).

⁵ J. F. Morin, J. P. Maita, H. J. Williams, R. C. Sherwood, J. H. Wernick, and J. E. Kunzler, *Phys. Rev. Lett.* **8**, 275 (1962).

⁶ P. S. Swartz, *J. Appl. Phys.* **34**, 1365 (1963).

⁷ J. Babiskin, P. G. Siebenmann, G. Otto, and E. Saur, *Z. Physik* **180**, 483 (1964).

⁸ D. B. Montgomery and H. Witzgall, *Phys. Lett.* **22**, 48 (1966).

⁹ D. L. Decker and H. L. Laquer, *Bull. Amer. Phys. Soc.* **11**, 345 (1966).

¹⁰ A. M. Clogston, *Phys. Rev. Lett.* **9**, 266 (1962).

¹¹ L. J. Neuringer and Y. Shapira, *Phys. Rev. Lett.* **17**, 81 (1966).

¹² N. R. Werthamer, E. Helfand, and P. C. Hohenberg, *Phys. Rev.* **147**, 295 (1966).

¹³ Y. B. Kim, C. F. Hempstead, and A. R. Strnad, *Phys. Rev. Lett.* **9**, 306 (1962); *Phys. Rev.* **129**, 528 (1963).

¹⁴ P. W. Anderson, *Phys. Rev. Lett.* **9**, 309 (1962).

¹⁵ H. L. Laquer, in Ref. 3, p. 156.

¹⁶ D. L. Decker, *Rev. Sci. Instrum.* **39**, 602 (1968).

¹⁷ L. A. Weber, D. E. Diller, H. M. Roder, and R. D. Goodwin, *Cryogenics* **2**, 236 (1962).

¹⁸ H. L. Laquer and D. L. Decker, *Cryogenics* **6**, 109 (1966).

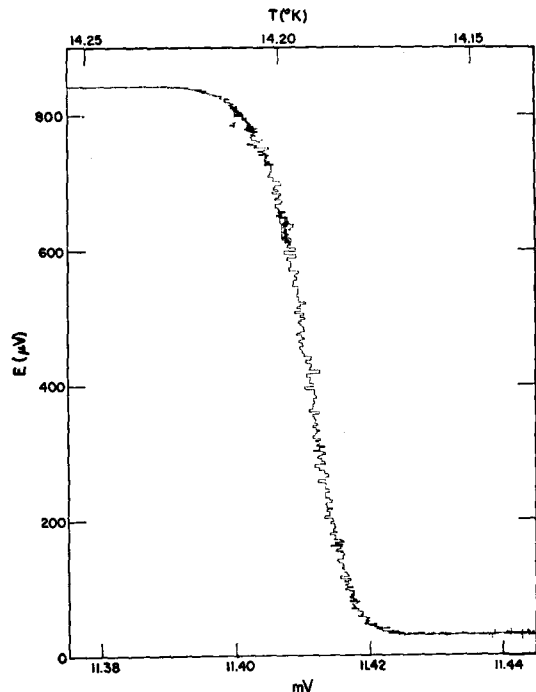


FIG. 1. Zero field transition at 100 kHz, 0.05 Oe p-p. Ac signal E from pickup coil as a function of carbon resistor thermometer voltage, mV, at a fixed measuring current of $103.5 \mu\text{A}$ (lower scale) and corresponding temperature T (upper scale). Steps are caused by 1-sec sampling period of digital voltmeter used for carbon thermometer readout.

stable to within $\pm 0.002^\circ\text{K}$ using an electronic bridge controller.¹⁹ The temperature of the sample was measured with an Allen-Bradley 0.1 W, 43- Ω carbon resistor. This resistor was calibrated using points in the helium vapor pressure range and it was also compared *in situ* with a germanium thermometer subsequently calibrated at the U. S. National Bureau of Standards.²⁰ The magnetoresistance of the carbon thermometer was measured in liquid helium and in liquid hydrogen and appropriate corrections were applied at intermediate temperatures. At 68 kOe and 12.2°K these corrections were equivalent to 79 mdeg.²¹ Our overall temperature accuracy is estimated to be ± 20 mdeg and the precision which enters in determining slopes ± 10 mdeg.

The V_3Ga cylinder was located inside a primary or drive coil which could be made to generate an ac field of 0.01 to 60 Oe peak to peak (p-p) for frequencies in the range from 40 Hz to 400 kHz. Inside the cylinder was a pickup coil, about 3 mm long wound with 500 turns of B & S #49 gauge (0.0025-cm-diam) Formex insulated copper wire. This assembly could be placed in either of the cryostats and positioned in the center of the high-field solenoid. The ac frequency and magnitude were preset and the signal from the pickup coil (amplified on a broad-band Hewlett Packard model 3400A voltmeter)

¹⁹ J. D. G. Lindsay, Rev. Sci. Instrum. **37**, 1192 (1966).

²⁰ G. Cataland and H. H. Plumb, J. Res. Nat. Bur. Stand. **70A**, 243 (1966).

²¹ D. L. Decker and H. L. Laquer (unpublished).

was recorded on an X-Y recorder at a given temperature while sweeping the dc field, or at a given dc field while slowly changing the temperature. Maximum noise level was always less than 10% of the normal state signal.

For the dc measurements two matched coils were used, one of which closely surrounded the V_3Ga sample. The coils were connected in opposition and the difference of the induced voltages was integrated by a Dymec model 2460A operational amplifier to give the amount of flux excluded from the coil containing the specimen. This difference was plotted against the magnetic field on an X-Y recorder. Due to residual thermal emf's in the circuit and the small size of our sample it was only possible to detect field differences greater than 1 G.

III. RESULTS

A typical zero-field transition using a 0.05 Oe (p-p), 100-kHz signal and sweeping the temperature at $0.002^\circ\text{K}/\text{min}$ is shown in Fig. 1. This transition is completely reversible with less than 0.002°K hysteresis. The full width of the transition from the point where the normal signal has dropped 0.5% to the point where the drop is 99.5% complete amounts to 0.056°K . This value represents an upper limit. A more generally accepted width value is obtained as the distance between the intercepts with the horizontal lines of the steep linear region of the transition curve (between the 1/4 and 3/4 completion points). This method of interpretation of the experimental data then yields a transition width of only 26 mdeg.

Several measurements of the normalized ac output signal against the dc field at constant temperature are shown in Fig. 2. These curves are also completely reversible, as long as the field is swept slowly so as to avoid heating the sample. Straight-line extrapolation gives a width of about 2.4 kOe for the transition as measured at the 0.05-Oe p-p ac level and noticeably greater values at the higher ac levels.

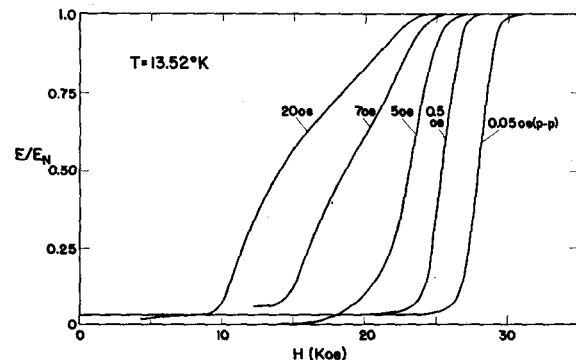


FIG. 2. Transitions in dc magnetic field for various ac levels at 13.52°K . Normalized ac signal from pickup coil, E/E_N , where E_N is the normal state limiting value of the ac signal E plotted as a function of the dc field H for various indicated values of the alternating field intensity.

Taking 0.5% changes in this output signal as reproducible decision levels, we obtain field values, H_N for the normal and H_S for the superconducting limit of the transition. Figure 3 shows the relation between H_S and the magnitude of the applied ac field. These are essentially critical current curves. For any given temperature there is a break or knee, indicated by the arrows, defining a field H_K . H_N also varies somewhat with the magnitude of the ac field, its maximum value $H_N(\text{max})$ being obtained with the smallest ac field. Since the midpoint field, where the output signal is one half of the normal state signal, can be determined with greater accuracy than either H_K or H_N , the field at the midpoint of the 100 kHz and 0.05-Oe (p-p) transitions was used to analyze the temperature dependence of the upper critical field and is thus designated as H_{c2} . The temperature variations of these various fields are shown in Fig. 4.

The dc measurements gave curves as shown in Fig. 5. The point of deviation from the Meissner line for the virgin curve, as indicated by the arrow in this figure, represents a maximum value for the lower critical field H_{c1} divided by $(1 - n)$, where $n = 0.2$ is our estimate of the demagnetizing factor. These experimental values of H_{c1} are plotted in Fig. 6. The slope of the dc magnetization curve near its upper end was so small that an accurate value of H_{c2} could not be determined. The width of the hysteresis, as in Fig. 5, is a measure of the

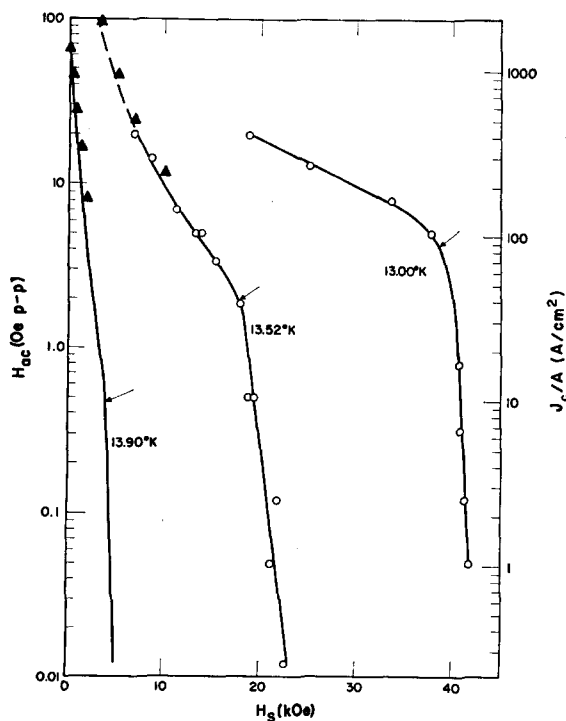


FIG. 3. Critical current curves. The maximum permissible alternating field intensity H_{ac} as a function of the lower threshold field H_S at various temperatures. Corresponding induced supercurrent densities are given by scale on right. The arrows indicate the position of the knee H_K . The solid triangles are taken from the dc measurements.

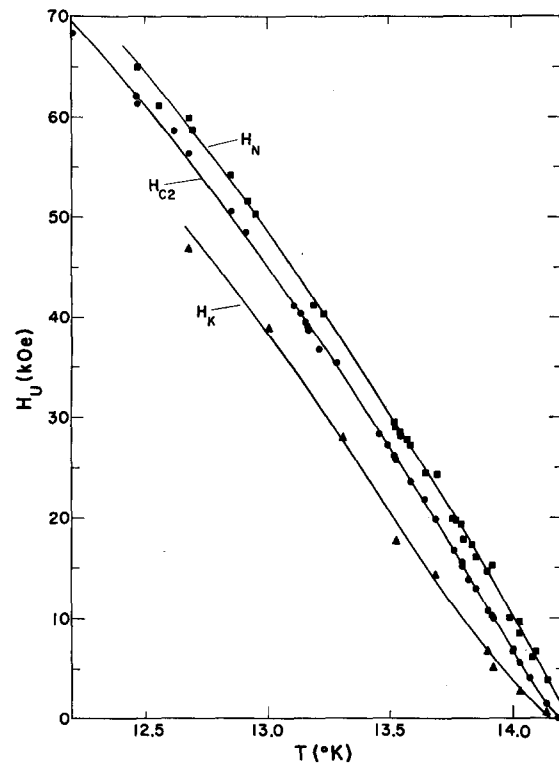


FIG. 4. Temperature variation of various upper critical fields. H_K represents the field at the knee of the critical current curves in Fig. 3. H_{c2} represents the midpoint of the "standard" 100-kHz, 0.05-Oe p-p transition. H_N represents the first indication of superconductivity.

maximum shielding currents and hence can be plotted with the ac critical current measurements in Fig. 3. Comparison between the ac and dc measurements is quite satisfactory in the range of validity of each.

IV. DISCUSSION

The measured zero-field transition width of 26 mdeg is narrower, by a factor of 72, than that predicted by Pippard's²² thermodynamic fluctuation theory for this material with a coherence length of 25 Å (see below). Actually, the true fluctuation-limited transition width is probably smaller than our measurements by a factor of 300 since the coherence length approaches the sample dimension at T_c as pointed out by Shier and Ginsberg.²³ Nevertheless, considering the type of material, our measured width indicates an acceptable homogeneity for the V_3Ga cylinder used in most of this study.

The dc magnetization curves are similar to those of other type II materials.¹³ The hysteresis pattern is symmetrical about the zero magnetization line because the specimen is multiply connected. Hence the hysteresis does not by itself imply irreversibility of the material. However, the absence of a sharp drop at the peak near H_{c1} as observed in reversible type II super-

²² A. B. Pippard, Proc. Roy. Soc. (London) **A203**, 210 (1950).

²³ J. S. Shier and D. M. Ginsberg, Phys. Rev. **147**, 384 (1966).

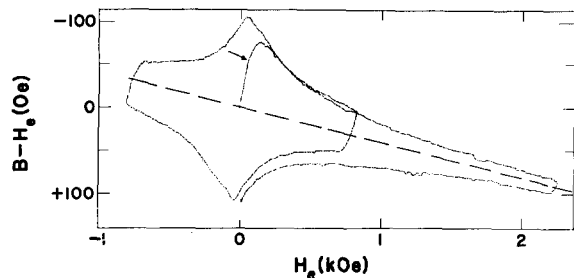


FIG. 5. Dc tube magnetization curve at 13.85°K. The zero magnetization axis (dashed line) is tilted due to a 2.8% mismatch in the two sensing coils. The final part of the curve does not close completely because of drifts from residual thermal emf's. (The slope of the Meissner region is not 45° because of the different scale factors used for the x and y axes and because of the demagnetizing factor.)

conductors²⁴ is an indication that even a singly connected sample of the identical material will exhibit considerable hysteresis. Since there are sizable shielding currents present above H_{c1} , its identification is difficult, and this together with the uncertainty in the demagnetizing factor leaves the determination of H_{c1} uncertain by $\pm 50\%$.

The ac method is far more sensitive than the dc and the measurements are readily interpreted in accordance with the tube magnetization experiments of Kim *et al.*¹³ Given a critical current density J_c , which is a function of the magnetic field, a tube wall thickness w , and a shape factor η , the maximum difference between the field inside and outside the tube is $\pm \eta J_c w$. Neglecting small frequency effects, there can be no ac signal within the cylinder until $2\eta J_c w$ is less than the p-p ac field, at which point the dc field equals H_S . For our sample geometry, complete shielding of a 0.01-Oe p-p field induces a critical current density of 208 mA/cm² if the current is uniformly distributed. On the other hand, at the high-field limit of the transition, only 0.5% of the ac signal is shielded with corresponding induced current densities of 1 mA/cm² at $H_N(\text{max})$.

One might be tempted to interpret the sudden drop in critical currents at H_K as the beginning of the bulk upper critical field transition and the field $H_N(\text{max})$ as the surface nucleation field H_{c3} .²⁵ If there were surface superconductivity we would expect $H_N(\text{max})$ to increase more rapidly than H_K with decreasing temperatures. However, their slopes are essentially the same except very near to T_c . If $H_N(\text{max})$ corresponded to H_{c3} the currents would flow only in a surface layer of the thickness of a coherence length which we calculate as 25 Å from the expression²⁶ $\xi \cong (\xi_0 l)^{1/2}$, where $\xi_0 = 52$ Å is the Bardeen-Cooper-Schrieffer²⁷ or BCS

²⁴ T. F. Stromberg and C. A. Swenson, Phys. Rev. Lett. **9**, 370 (1962).

²⁵ D. Saint-James and P. G. de Gennes, Phys. Lett. **7**, 306 (1963).

²⁶ P. G. de Gennes, *Superconductivity of Metals and Alloys* (W. A. Benjamin, Inc., New York, 1966), p. 225.

²⁷ J. Bardeen, L. N. Cooper, and J. R. Schrieffer, Phys. Rev. **108**, 1175 (1957).

coherence distance and $l = 12$ Å is the electron mean free path estimated from the normal state resistivity $\rho_n = 36 \mu\Omega \text{ cm}$.²⁸ The surface layer under these conditions would carry a current density of 160 A/cm². At any rate, since the slopes are the same, we have no evidence for surface superconductivity in our specimen which leaves us with the following possibilities: (a) there is no surface nucleation in $V_3\text{Ga}$, (b) the net current capacity of the surface layer is less than 160 A/cm², or (c) more specialized surface preparation methods than presently available are needed to exhibit surface superconductivity in $V_3\text{Ga}$.

Since the temperature dependence of all the curves in Fig. 4 is essentially the same, we are justified in choosing the most accurately measured one, H_{c2} , to calculate other properties of $V_3\text{Ga}$. The upper critical field increases so rapidly near T_c that our measurements only extend to a reduced temperature of 0.86. This range and the precision of our data, however, are sufficient to determine both the initial-slope and curvature of the upper critical field versus temperature curve, and hence the parameters α and λ_{s0} which have been used in recent theories to characterize type II superconductors.

The first of these,

$$\alpha = \sqrt{2} H_{c2}^*(0) / H_P(0), \quad (1)$$

was defined by Maki²⁹ in his theory of the upper critical field for a "dirty" superconductor including the effects of Pauli spin paramagnetism in the normal state, where $H_P(0)$, introduced by Clogston,¹⁰ represents the hypothetical critical field in the absence of all magnetization effects other than spin paramagnetism, and $H_{c2}^*(0)$ the GLAG³⁰ upper critical field, both at the absolute zero.

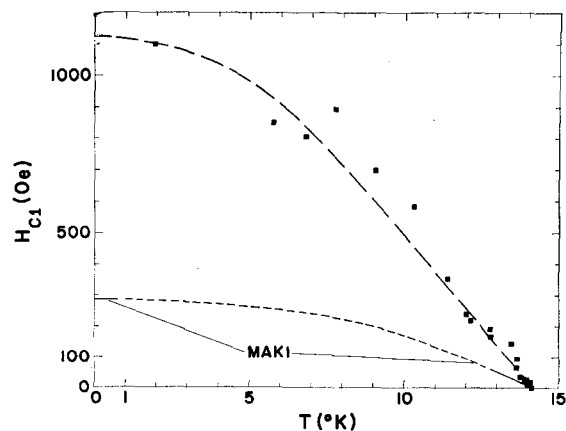


FIG. 6. Temperature variation of lower critical field. ■ Experimentally from break of Meissner line. — Calculated from Maki's relations using the experimental value of κ .

²⁸ N. B. Sarachik, G. E. Smith, and J. H. Wernick, Can. J. Phys. **41**, 1542 (1963).

²⁹ K. Maki, Physics **1**, 127, 201 (1964).

³⁰ V. L. Ginzburg and L. D. Landau, Zh. Eksp. Teor. Fiz. **20**, 1064 (1950); A. A. Abrikosov, *ibid.* **32**, 1442 (1957); L. P. Gor'kov, *ibid.* **37**, 1407 (1959).

The second or spin-orbit scattering parameter λ_{so} was introduced by Werthamer *et al.*¹² in their more general treatment which includes the compensatory paramagnetic lowering of the free energy of the superconducting state due to spin orbit scattering. They give

$$-\ln t = \sum_{n=-\infty}^{\infty} \left\{ |2n+1|^{-1} - \left[|2n+1| + \frac{\hbar}{t} + \frac{(\alpha\hbar/t)^2}{|2n+1| + (\hbar + \lambda_{so})/t} \right]^{-1} \right\}, \quad (2)$$

with the dimensionless variables t , \hbar , α , and λ_{so} as defined in Eq. (27) of their paper.

We have obtained an expansion of Eq. (2) valid for T near T_c in which we let $\theta = 1 - t \ll 1$. This expansion to order θ^2 yields

$$\hbar = A'\theta(1 - B\theta), \quad (3)$$

with

$$A' = \pi^2/4 \quad (4)$$

and

$$B = \frac{1}{2} - (28/\pi^4)\zeta(3) + (16\alpha^2/\pi^4\lambda_{so}) \times \left\{ \frac{1}{4}\pi^2 - \lambda_{so}^{-1} [\psi(\frac{1}{2}\lambda_{so} + \frac{1}{2}) - \psi(\frac{1}{2})] \right\}, \quad (5)$$

where the Riemann function $\zeta(3) = 1.202$ and $\psi(z)$ is the digamma function.³¹

There are two methods of obtaining α discussed by Werthamer *et al.*¹² One follows from the experimental slope of H_{c2} near T_c

$$\alpha = 5.2758 \times 10^{-5} (-dH_{c2}/dT)_{T_c}, \quad (6)$$

and the other involves experimental data on the normal state, which in the short mean-free path or "dirty" limit gives

$$\alpha = 3e^2\hbar\gamma\rho_n/2m\pi^2k_B^2, \quad (7)$$

where γ and ρ_n are the normal state electronic specific heat and electrical resistivity, respectively, and the remaining quantities are fundamental constants. The value of $\gamma = 3.04 \times 10^4$ erg cm⁻³ deg⁻² is taken from Morin *et al.*⁵ and $\rho_n = 36 \mu\Omega$ cm from Sarachik *et al.*²⁸

Our experimental data can be fitted to an equation of the form

$$H_{c2}(T) = A\theta(1 - B\theta) \quad (8)$$

by a least-squares analysis with $A = 612 \pm 8$ kOe, $B = 1.27 \pm 0.10$, and $T_c = 14.16 \pm 0.01^\circ\text{K}$. This value of T_c is 0.03°K below the measured value of 14.19°K because of a narrow region of positive curvature for $T/T_c > 0.985$ which cannot be accommodated by Eq. (8). The parameters reproduce the measured field values with an rms deviation of 0.55 kOe. From these experimental values of A , B , and T_c the slope of H_{c2} at T_c , α , and λ_{so} are obtained using Eqs. (5) and (6).

TABLE I. Summary of results.

$T_c(\text{meas}) = 14.19 \pm 0.02^\circ\text{K}$	$H_P(0) = 260$ kOe
$(dH_{c2}/dT)_{T_c} = -43.2 \pm 0.7$ kOe/ $^\circ\text{K}$	$H_{c2}^*(0) = 420$ kOe
$\alpha[\text{Eq. (6)}] = 2.28 \pm 0.04$	$H_{c2}(0) = 270 \pm 60$ kOe
$\alpha[\text{Eq. (7)}] = 2.65$	$\kappa[\text{Eq. (9)}] = 40 \pm 2$
$\lambda_{so} = 0.6 \pm 0.1$	$\kappa[\text{Eq. (10)}] = 48 \pm 5$

The results are given in Table I with the statistical errors representing one mean deviation.

Our initial slope near T_c of -43.2 ± 0.7 kOe/deg can be compared with Wernick *et al.*'s³ -53 kOe/deg and Montgomery and Witzgall's⁸ -39.1 kOe/deg both from direct resistance measurements and Morin *et al.*'s⁵ -48 kOe/deg from specific heat data.

The value of κ can also be estimated in two ways, both, however, involving the normal state electronic specific heat. From the definition $H_{c2} = \sqrt{2}\kappa H_c$ and the slope $(dH_c/dT)_{T_c} = 4.405\gamma^{1/2}$ given by BCS²⁷ one finds

$$\kappa = 0.1605\gamma^{-1/2}(-dH_{c2}/dT)_{T_c}. \quad (9)$$

Goodman³² and Berlincourt³³ estimate a value of κ from the electronic properties of the normal metal. The major contribution arises from

$$\kappa_l = 7.53 \times 10^3 \rho_n \gamma^{1/2}, \quad (10)$$

where ρ_n is in Ω cm. The results for κ are also tabulated in the table.

A limiting expression for Eq. (2) valid at $T=0$ is given by Werthamer *et al.*¹² as

$$2.54 = -\ln K + (\lambda_{so}/\delta) \tan^{-1}[\delta/(\hbar + \frac{1}{2}\lambda_{so})], \quad (11)$$

where $K = \{(1 + \alpha^2)\hbar^2 + \lambda_{so}\hbar\}$, $\delta = \{a^2\hbar^2 - \frac{1}{4}\lambda_{so}\}^{1/2}$, and $\hbar = H_{c2}(0)/3.56H_{c2}^*(0)$.³⁴ If we take $H_P(0) = 18400T_c$ ¹⁰ and the α calculated from experimental results near T_c , the value of $H_{c2}^*(0)$ can be calculated from Eq. (1). Then from the values of λ_{so} and α determined near T_c we use Eq. (11) to calculate $H_{c2}(0)$. These results are given in the table. Our calculated $H_{c2}(0)$ of 270 ± 60 kOe is somewhat larger than the 208 ± 5 kOe reported by Montgomery and Witzgall⁸ from measurements at 4°K on very similar material. However, the agreement is within the estimated errors, which is quite satisfactory, considering the limitations of the present theories, the small range of reduced temperatures covered in our measurements and the extent of our extrapolation.

Finally, using the experimental value for κ and Maki's²⁹ expression for the lower critical field, $H_{c1}(T)$ one can calculate $H_{c1}(T)$ and compare it with the results from the dc magnetization measurements. This comparison is shown by the calculated curve for H_{c1} in Fig. 6. It should be noted that the calculated H_{c1} is less than

³² B. B. Goodman, IBM J. Res. Develop. **6**, 63 (1962).

³³ T. G. Berlincourt and R. R. Hake, Phys. Rev. **131**, 140 (1963).

³⁴ S. J. Williamson, Phys. Lett. **23**, 629 (1966).

³¹ *Handbook of Mathematical Functions*, M. Abramowitz and I. A. Stegun, Eds. (National Bureau of Standards Applied Mathematics Series, Washington, D.C., 1964), p. 258.

1/3 of the experimental points. This discrepancy may well be due to the difficulty of determining the break from the linear Meissner region due to trapped shielding currents which cause the experimenter to overestimate H_{c1} . Even the results on 70- μ powders by Swartz *et al.*⁶ gave an H_{c1} lower than our experimentally estimated H_{c1} , but greater than the calculated value.

V. CONCLUSIONS

The ac method of measuring magnetization and the interpretation thereof described in the paper is in good agreement with more standard dc techniques but is considerably more sensitive in the region near H_{c2} where the magnetic moment is small. Given material with a sufficiently narrow transition, and thermometry of sufficient accuracy, our technique yields values for the slope as well as for the initial curvature of the upper critical field as a function of the temperature. These experimental numbers are then used together with the current theories to calculate more derived quantities, including a reliable value for the parameter α , and an

estimate for the spin orbit scattering parameter in the superconducting state.

The dc measurements emphasize the great difficulty of accurately determining H_{c1} in a massive specimen of nonideal type II superconductor in which there are considerable shielding currents in the region above H_{c1} .

It is conceivable that there may be metallurgical differences between V_3Ga samples used by different investigators. Nevertheless, wherever a comparison is possible, the properties of the V_3Ga used in this study are not significantly different from those reported by others.

ACKNOWLEDGMENTS

We wish to thank Professor B. T. Matthias for supplying the V_3Ga samples and encouraging us in this work and Dr. L. Gruenberg for a number of enlightening discussions. One of us also is grateful to Dr. E. F. Hammel and the cryogenics group at Los Alamos for the hospitality extended to him there as a Visiting Staff Member during his sabbatical leave.

Equivalent Circuit of a Superconducting Bolometer*

M. K. MAUL† AND M. W. P. STRANDBERG

Departments of Electrical Engineering and Physics and Research Laboratory of Electronics, Massachusetts Institute of Technology, Cambridge, Massachusetts 02139

(Received 18 November 1968; in final form 25 February 1969)

The theory of superconducting bolometer operation is presented and a small-signal equivalent circuit developed. This circuit contains a portion that represents dynamic thermal effects and a portion resulting from superconductive phenomena. It is shown that the incremental impedance is greater than the dc resistance even for the limit of zero-frequency modulation. A peaking phenomenon is predicted in the incremental impedance versus temperature for this circuit. The characteristic parameters of a tin superconducting bolometer are presented to indicate the usefulness of incremental impedance measurements in determining these parameters.

I. INTRODUCTION

Superconducting films have been shown to be fast sensitive detectors at frequencies from the microwave region to the near infrared.^{1,2} The large variation of resistance with temperature at the superconducting transition enables one to construct a device with high responsivity. The small mass of the evaporated film and the small specific heat at low temperatures make possible thermal time constants of 15–25 nsec. The

operation at low temperatures also reduces the noise equivalent power (NEP).

Although the bolometric properties of the superconducting-to-normal transition have been recognized since 1946,³ there has been little application until recently. A thin-film bolometer with a time constant τ of 1 sec and an NEP of 10^{-13} W/Hz^{1/2} has been used in the range 1 mm–70 μ .¹ The microwave properties have been discussed by Bertin and Rose.² Moreover, the superconducting bolometer has been used for detection of microwave phonons at MIT.⁴

Additional work at MIT has proceeded in a somewhat different direction. The noise properties of the device have been investigated. Furthermore, the

* This work was supported principally by the Joint Services Electronics Program [Contract DA 28-043-AMC-02536(E)]. It is based on a thesis by M. K. M. submitted to the Massachusetts Institute of Technology in partial fulfillment of the requirements for the degree of Doctor of Philosophy in Electrical Engineering.

† Present address: Bell Telephone Laboratories, Inc., Murray Hill, N.J. 07974.

¹ D. Bloor, T. Dean, G. Jones, D. Martin, P. Mower, and C. Perry, Proc. Roy. Soc. (London) **A260**, 510 (1961).

² C. L. Bertin and K. Rose, J. Appl. Phys. **39**, 2561 (1968).

³ D. H. Andrews, R. M. Milton, and W. DeSorbo, J. Opt. Soc. Amer. **36**, 518 (1946).

⁴ J. M. Andrews, Jr., and M. W. P. Strandberg, Proc. IEEE **54**, 523 (1966).